INTERNATIONAL JOURNAL OF OPTIMIZATION IN CIVIL ENGINEERING
Int. J. Optim. Civil Eng., 2018; 8(2):181-194

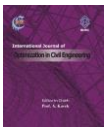

ESTIMATING DRYING SHRINKAGE OF CONCRETE USING A MULTIVARIATE ADAPTIVE REGRESSION SPLINES APPROACH

A. Kaveh[1*, †], S. M. Hamze-Ziabari[1] and T. Bakhshpoori[2]
[1]*Centre of Excellence for Fundamental Studies in Structural Engineering, Iran University of Science and Technology, Tehran-16, Iran*
[2]*Faculty of Technology and Engineering, Department of Civil Engineering, East of Guilan, University of Guilan, Rudsar-Vajargah, Iran*

ABSTRACT

In the present study, the multivariate adaptive regression splines (MARS) technique is employed to estimate the drying shrinkage of concrete. To this purpose, a very big database (RILEM Data Bank) from different experimental studies is used. Several effective parameters such as the age of onset of shrinkage measurement, age at start of drying, the ratio of the volume of the sample on its drying surface, relative humidity, cement content, the ratio between water and cement contents, the ratio of sand on total aggregate, average compressive strength at 28 days, and modulus of elasticity at 28 days are included in the developing process of MARS model. The performance of MARS model is compared with several codes of practice including ACI, B3, CEB MC90-99, and GL2000. The results confirmed the superior capability of developed MARS model over existing design codes. Furthermore, the robustness of the developed model is also verified through sensitivity and parametric analyses.

Keywords: prediction; drying shrinkage; concrete; multivariate adaptive regression splines (MARS).

Received: 17 June 2017; Accepted: 12 August 2017

1. INTRODUCTION

Mechanical properties of materials stand as one of the most important indicators for evaluating the strength and serviceability of reinforced concrete structures. Among these

[*]Corresponding author: Centre of Excellence for Fundamental Studies in Structural Engineering, Iran University of Science and Technology, Tehran-16, Iran
[†]E-mail address: alikaveh@iust.ac.ir (A. Kaveh)

properties, long-term properties of concrete that are mainly affected by the secondary influences of creep and shrinkage are of great importance to a structural engineer. Appropriate predictions of creep and shrinkage are very crucial tasks to assess the risk of concrete cracking, and deflection due to stripping-reshoring [1]. Therefore, presenting and developing a robust predictive model for both creep and shrinkage seem to be necessary.

There are several types of shrinkage distinguished depending on the cause of moisture loss. In this study, the drying shrinkage, which is defined as the removal of observed water from the hydrated cement paste when it is exposed to the environment, is investigated. Drying shrinkage problem is very complex phenomena and several parameters involved in this problem. The temperature and availability of water during curing, the environmental humidity and temperature after curing, the composition of the concrete, and the mechanical properties of the aggregates are the main parameters effect on shrinkage. Developing a user-friendly relationship between the drying shrinkage and parameters involved in this problem is still controversial in civil engineering.

Various codes of practice like ACI 209R-92 [1], B3 by Bazant-Baweja [2], CEB MC90-99 [3], and GL2000 [4] are presented to predict shrinkage in concrete. The ACI model is only applicable to normal weight and all the lightweight concretes under the standard conditions. The CEB-FIP model is also restricted to ordinary structural concretes with 28 days mean cylinder compressive strength varying from 12 to 80 MPa, mean relative humidity 40%-100% and mean temperature 5-30 ºC. The B3 model, which is an improved version of the earlier models namely BP model [5-8] and BP-KX model [9, 10], is restricted to the Portland cement concretes with a 28-days mean cylinder compressive strength varying from 17 to 70 MPa, W/C ratio 0.30-0.85, a/c ratio 2.5-13.5 and cement content 160-720 kg/m3. The GL2000 model, which is a modified form of the earlier GZ model by Gardner and Zhao [4], is also only applicable to concrete with characteristic strength less than 70 MPa and W/C ratio between 0.40 and 0.60. Goel et al. [11] evaluated the performances of the mentioned models based on RILEM (International Union of Laboratories and Experts in Construction Materials) database. Results indicated that the ACI, the B3, the CEB-FIP, and the GL2000 models underestimate the experimental shrinkage for all the concrete grades and there are significant scatters between predicted values and observed ones. In fact, the variability of shrinkage test measurements prevents models from closely matching experimental data [1].

In recent years, soft computing approaches have been introduced as reliable methods for developing predictive models in civil engineering problems (e.g. [12-18]). Artificial neural networks (ANNs) are known as the most popular soft computing approaches. In this regard, Bal and Buyle-Bodin [19] developed a multi-layer perceptron neural networks to estimate the drying shrinkage of concrete. The results of their study confirm the superior predictive ability of developed ANN model in comparison with the mentioned design codes in the previous paragraph. However, ANN model suffers from several drawbacks. For instance, the selection of structures of such networks is completely random and several models should be performed to obtain an appropriate configuration. Furthermore, ANNs do not present a definite function to estimate the response values based on input variables.

The main purpose of this study is to use the multivariate adaptive regression splines (MARS) algorithms for improving the predictive capability in the estimation of drying shrinkage in concrete. The MARS algorithm is a high-precision technique which was firstly

introduced by Friedman [20]. The main advantage of MARS model in comparison with ANN model is that the relationship between input and output variables is completely known and the user can easily estimate the response variable for a set of input variables. To develop a new predictive model, a comprehensive big database extracted from the RIELM databank [21] is applied. The results of the developed model are compared with different codes of practice based on statistical error parameters. Furthermore, the effects of different predictive variables are investigated through sensitivity and parametric analyses.

The remaining sections of the paper are organized as follows. In Section 2, the MARS algorithms are outlined. Section 3 describes the dataset used and also the process of modeling. The performance of proposed models, the parametric and sensitivity analyses are presented in Section 4. At the end, the paper is concluded in Section 5.

2. METHODOLOGY

There are two major categories for model trees: (a) Multiple Adaptive Regression spline (MARS) and (b) M5 model tree methods. In this research, MARS methods have been used for predicting drying shrinkage. For practical problems with the numeric variable response, the Regression Model Tree is usually applied because it has a numeric value rather than a class label linked to each leaf or classification. Model trees are quite similar to regression trees but it connects leaves with multivariate linear models. For problems dealing with continuous classes of variables, model tree technique has been successfully applied. The model tree offers a formational depiction of the data and piecewise linear fit to members of each class is calculated. In a model tree, there is a linear function assigned to each leaf, and no discretization of class labels is needed while it keeps conventional tree structure. Model trees are more accurate than regression trees while they are much smaller in size.

2.1 Overview of multivariate adaptive regression splines (MARS)

MARS is a novel approach in the field of data mining that models the nonlinear relationship between inputs and output variables using a series of piecewise linear or cubic segments (splines). These splines divide the space of input parameters into various subspaces and the algorithm fits a spline function in each subspace, which is known as basis functions (BFs). The basis function and its slope in each subspace can be changed from one subspace to the neighbor subspace. The end points of each segment are called knots. In other words, a knot determines the end of one region of data and the beginning of another. Unlike the well-known parametric linear regression analysis, MARS provides greater flexibility to explore nonlinear relations between a response variable and input variables. Furthermore, MARS also searches all possible interactions between variables by checking all degrees of interactions. The algorithm considers all functional forms and interactions between input variables, and therefore, it can effectively track the complex structures existing in data points and hidden relationships in a high-dimensional dataset. The general form of MARS model is defined as follows [20]:

$$\tilde{f}(x) = \beta_0 + \sum_{m=1}^{M} \beta_m \lambda_m(x) \tag{1}$$

where $\tilde{f}(x)$ is the predicted response, β_0 and β_m are parameters which are estimated to yield the best data fit and m is the number of BFs included into the model. The basis function in MARS model can be either one univariable spline function, or a product of two or more spline functions for different predictor variables. The spline BF, $\lambda_m(x)$, can be specified as:

$$\lambda_m(x) = \prod_{k=1}^{k_m} [s_{km}(x_{v(k,m)} - t_{k,m})] \tag{2}$$

where k_m is the number of knots, s_{km} takes either 1 or -1 and indicates the right/left regions of the associated step function, $v(k,m)$ is the label of the predictor variable and $t_{k,m}$ is the knot location.

MARS produces the BFs based on a stepwise procedure in whole searching space. The locations of knots are determined according to an adaptive regression algorithm. An optimal MARS is developed through a two-stage forward and backward procedure. In the forward stage, MARS over-fits data by considering a great number of BFs. In the backward, to avoid overfitting, redundant BFs are deleted from equation (1). MARS adopts Generalized Cross-Validation (GCV) criterion to remove the redundant BFs. The expression of GCV is as follow [20]:

$$GCV = \frac{\frac{1}{N}\sum_{i=1}^{N}\left[y_i - \hat{f}(x_i)\right]^2}{\left[1 - \frac{C(B)}{N}\right]^2} \tag{3}$$

in which N is the number of data points, and $C(B)$ is a complexity penalty that increases with the number of BFs in the model, and it is defined as:

$$C(B) = (B+1) + dB \tag{4}$$

where d is a penalty for each BF included into the model and B is a number of BFs.

3. DEVELOPMENT OF MARS MODEL

In this study, the MARS algorithm was developed to predict the drying shrinkage using the following steps.

3.1 Model inputs and outputs

Nine variables were presented to the MARS as model inputs including the age of onset of

shrinkage measurement (t), age at start of drying (t_c), the ratio of the volume of the sample on its drying surface (V/S), relative humidity (RH), cement content (C), the ratio of water content and cement content (W/C), the ratio of sand on total aggregate (a/c), average compressive strength at 28 days (f_{cm28}), and modulus of elasticity at 28 days (E_{cm28}). The single model output is the drying shrinkage (S). The histograms of input and output variables are presented in Fig. 1. As shown, the database used covers a wide range of cement content, W/C, and f_{cm28}. It should be noted that the developed model can be more reliable in ranges which data points are more concentrated.

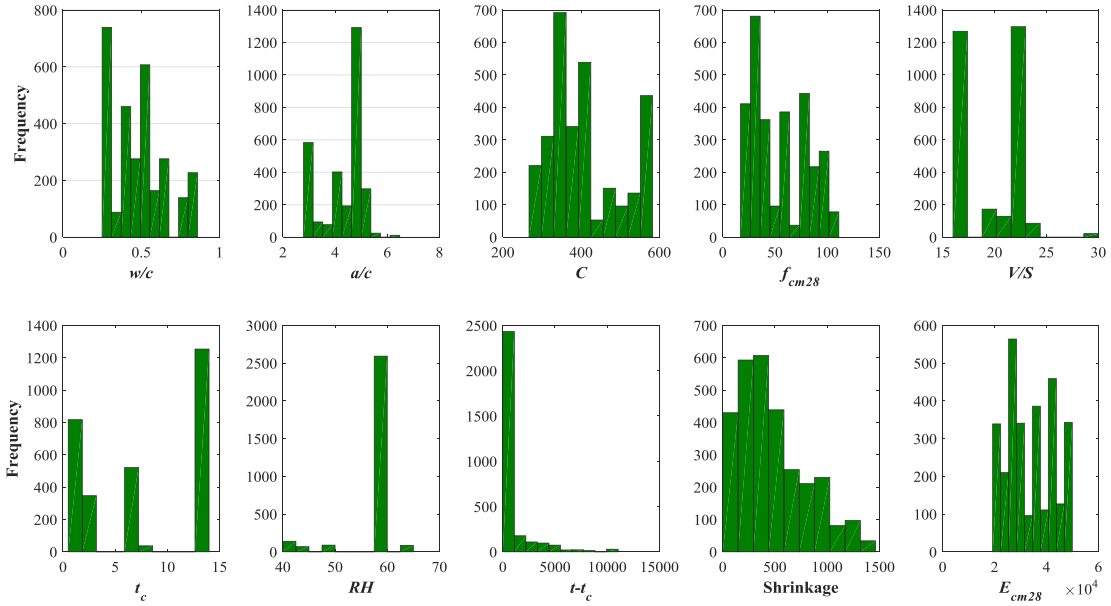

Figure 1. Histograms of input and output variables

3.2 Data division and Pre-processing

The data used to calibrate and validate the MARS model were obtained from RILEM (the International Union of Laboratories and Experts in Construction Materials) database, including shrinkage tests carried out in various laboratories. To develop a new model using MARS algorithm, the available data were randomly divided into training and testing subsets. The training data were taken for the learning procedure of the algorithm. The testing datasets were used to specify the generalization capability of the models to a new data they did not train with. In other words, the testing data were employed to measure the performance of the models obtained by MARS algorithm when applied to a dataset which played no role in building the models. The statistical parameters of the considered effective variables for training and testing subsets are presented in Table 1, which include the mean, standard deviation, minimum, maximum and range. From this table, it can be seen that the ranges of input parameters for both training and testing stages are notably wide. Therefore, it can be expected that the derived models would potentially provide better predictions for the cases, especially, where the densities of data points are higher. Out of the 2977 data, 2382 data vectors (80%) were taken for the training process. The remaining 595 data (20%) were used for the testing of the models.

Table 1: The statistical parameters of the input variables for training and testing datasets

Parameter	Subsets	Min	Max	Mean	Std.
W/C	Training	0.25	0.86	0.47	0.16
	Testing	0.25	0.86	0.48	0.16
a/c	Training	2.79	6.48	4.28	0.81
	Testing	2.79	6.48	4.27	0.80
f_{cm28}	Training	17	111.3	54.84	27.05
	Testing	17	111.3	52.41	26.35
E_{cm28}	Training	19276.99	49943.14	33939.32	8790.09
	Testing	19276.99	49943.14	33173.6	8631.21
RH	Training	40	65	58.59	5.03
	Testing	40	65	58.42	5.15
V/S	Training	16	30	19.88	2.64
	Testing	16	30	19.67	2.56
t_c	Training	0.5	14	7.72	5.69
	Testing	0.5	14	8.07	5.69
Δt	Training	0.03	11056.6	785.65	1739.89
	Testing	0.06	10882.1	786.23	1718.55
C	Training	267	583	411.6	92.40
	Testing	267	583	411.83	92.43

In the knowledge discovery approaches such as ANN, before data mining itself, data pre-processing plays a crucial role. The normalization of the data is one of the first steps in data mining approaches. This step is very important when dealing with parameters of different units and scales. Therefore, all parameters considered for estimating shrinkage are normalized between 0 and 1 to have the same scale for a fair comparison between them.

3.3 Developed model

After the data division step, the training dataset is presented to the MARS algorithm. The MARS model provides a predictive model as the general form of Eq. (5) for estimation of drying shrinkage. The extended form of MARS model is presented in Table 2. According to this table, the developed model is consists of 59 basis functions. The developed MARS model captures complex relationships between input and output variables without an additional effort to verify a priori assumption about the relationship between the set of input variables and output response variable. This feature of MARS model can be more practical as the dimension of the problem increases.

$$S = 5.3 + 240BF_1 - 250BF_2 + 15BF_3 + 2.5BF_4 - 73BF_5 - 190BF_6 + 0.59BF_7 - 120BF_8 + 0.64BF_9 + 1.6BF_{10} - 11BF_{11} - 160BF_{12} + 110BF_{13} - 60BF_{14} + 830BF_{15} + 1.8BF_{16} + 970BF_{17} + 510BF_{18} - 2BF_{19} - 75BF_{20} - 44BF_{21} + 120BF_{22} + 32BF_{23} + 1.5BF_{24} - 1.5\times10^4 BF_{25} + 98BF_{26} - 120BF_{27} + 110BF_{28} + 0.48BF_{29} - 3.5BF_{30} - 1.7BF_{31} + 34BF_{32} - 22BF_{33} - 3BF_{34} - 430BF_{35} - 290BF_{36} + 150BF_{37} + 2.4\times10^3 BF_{38} + 25BF_{39} - 3.5BF_{40} - 9.1BF_{41} + 440BF_{42} + 51BF_{43} + 48BF_{44} + 1.6\times10^4 BF_{45} - 36BF_{46} + 40BF_{47} - 140BF_{48} + 97BF_{49} - 120BF_{50} + 44BF_{51} - 46BF_{52} - 26BF_{53} - 3.2BF_{54} - 9.1\times10^4 BF_{55} + 410BF_{56} + 35BF_{57} + 600BF_{58} + 130BF_{59} \quad (5)$$

Table 2: The list of basis functions and their equations

Bf no.	Equation	Bf no.	Equation
BF_1	max(0, Δt -0.022)	BF_{31}	BF_3 * max(0, 0.29 - *V/S*)
BF_2	max(0, 0.022 -Δt)	BF_{32}	BF_{13} * max(0, *C* -0.74)
BF_3	max(0, *W/C* -0.049)	BF_{33}	BF_{13} * max(0, 0.74 - *C*)
BF_4	max(0, 0.049 - *W/C*)	BF_{34}	BF_{10} * max(0, E_{cm28} -0.3)
BF_5	BF_3 * max(0, E_{cm28}-0.0021)	BF_{35}	BF_{10} * max(0, 0.3 - E_{cm28})
BF_6	BF_3 * max(0, 0.0021- E_{cm28})	BF_{36}	BF_{34} * max(0, 0.42 - f_{cm28})
BF_7	BF_3 * max(0, Δt -0.0023)	BF_{37}	max(0, 0.0015 -Δt) * max(0, *a/c* -0.035)
BF_8	BF_3 * max(0, 0.0023 -Δt)	BF_{38}	max(0, 0.0015 -Δt) * max(0, 0.035 - *a/c*)
BF_9	max(0, t_c -0.19)	BF_{39}	BF_{23} * max(0, *V/S* -0.36)
BF_{10}	max(0, 0.19 - t_c)	BF_{40}	BF_{14} * max(0, t_c -0.037)
BF_{11}	BF_2 * max(0, *a/c* -0.068)	BF_{41}	BF_{16} * max(0, 0.24 -Δt)
BF_{12}	BF_2 * max(0, 0.068 - *a/c*)	BF_{42}	BF_{15} * max(0, 0.26 -Δt)
BF_{13}	BF_3 * max(0, f_{cm28} -0.12)	BF_{43}	max(0, 0.022 -Δt) * max(0, t_c -0.037) * max(0, *a/c* - 0.41)
BF_{14}	BF_5 * max(0, f_{cm28}-0.064)	BF_{44}	max(0, 0.022 -Δt) * max(0, t_c -0.037) * max(0, 0.41 - *a/c*)
BF_{15}	BF_5 * max(0, 0.064 - f_{cm28})	BF_{45}	BF_{25} * max(0, 0.12 -Δt)
BF_{16}	BF_9 * max(0, *C* -0.44)	BF_{46}	BF_{28} * max(0, *C* -0.38)
BF_{17}	max(0, *W/C* -0.049) * max(0, 0.12 -f_{cm28}) * max(0, E_{cm28} -0.062)	BF_{47}	max(0, Δt -0.0015) * max(0, *RH* -0.2) * max(0, 0.38 - *C*) * max(0, 0.17 - E_{cm28})
BF_{18}	max(0, *W/C* -0.049) * max(0, 0.12 - f_{cm28}) * max(0, 0.062 - E_{cm28})	BF_{48}	max(0, Δt -0.00047)
BF_{19}	BF_9 * max(0, E_{cm28}-0.21)	BF_{49}	BF_{48} * max(0, 0.4 - *RH*)
BF_{20}	BF_9 * max(0, 0.21- E_{cm28})	BF_{50}	BF_{27} * max(0, *RH* -0.4)
BF_{21}	BF_9 * max(0, 0.0064 -Δt)	BF_{51}	max(0, *W/C* -0.049) * max(0, 0.12 - f_{cm28}) * max(0, Δt - 0.55)
BF_{22}	BF_2 * max(0, 0.037 - t_c)	BF_{52}	max(0, *W/C* -0.049) * max(0, 0.12 - f_{cm28} * max(0, 0.55 -Δt)
BF_{23}	BF_{14} * max(0, 0.96 - *C*)	BF_{53}	BF_7 * max(0, 0.22 - E_{cm28})
BF_{24}	BF_{19} * max(0, f_{cm28} -0.15)	BF_{54}	max(0, 0.21 - f_{cm28})
BF_{25}	BF_{19} * max(0, 0.15 - f_{cm28})	BF_{55}	BF_{37} * max(0, 0.0021 - E_{cm28})
BF_{26}	max(0, t_c -0.19) * max(0, 0.44 - *C*) * max(0, 0.16 - f_{cm28})	BF_{56}	BF_{32} * max(0, E_{cm28} -0.78)
BF_{27}	max(0, x8 -0.0015)	BF_{57}	BF_{46} * max(0, t_c -0.037)
BF_{28}	BF_{27} * max(0, *RH* -0.2)	BF_{58}	BF_{46} * max(0, 0.037 - t_c)
BF_{29}	max(0, f_{cm28} -0.2)	BF_{59}	BF_{28} * max(0, 0.13 - *W/C*)
BF_{30}	BF_3 * max(0, *V/S* -0.29)		

To analytically evaluate the performances of the developed models, the following statistical error parameters were applied: BIAS, root mean square error (*RMSE*), correlation coefficient (*R*) and coefficient of determination (R^2).

$$BIAS = \frac{\sum_{i=1}^{N}(P_i - O_i)}{N} \tag{6}$$

$$RMSE = \sqrt{\frac{1}{N}\sum_{i=1}^{N}(P_i - O_i)^2} \tag{7}$$

$$R = \frac{\sum_{i=1}^{N}(P_i - P_m)(O_i - O_m)}{\sqrt{(P_i - P_m)^2}\sqrt{(O_i - O_m)^2}} \tag{8}$$

$$R^2 = 1 - \frac{\sum_{i=1}^{N}(O_i - P_i)^2}{\sum_{i=1}^{N}(O_i - O_m)^2} \tag{9}$$

where O_i is the measured value, P_i stands for prediction values, N is the number of data points, O_m is the mean value for observation, and P_m is the mean value of prediction.

4. RESULTS AND DISCUSSIONS

The performance of MARS model in the training and testing sets are illustrated in Fig. 2, which presents the scatter between measured and predicted drying shrinkage around the optimal line of equality. As shown, there is a little scatter around the optimal line between predicted and measured values of drying shrinkage in both training and testing sets. The similar performances of the MARS model on the training and testing data indicate that they have both good predictive ability and generalization performances. The MARS model performance is further confirmed analytically in Table 3, which contains four different performance measures including the coefficient of correlation, *R*, the coefficient of determination (or efficiency), R^2, root mean square error, *RMSE*, and *BIAS*. Smith [22] stated that if the correlation coefficient is more than 0.8, there is a strong correlation between measured and predicted values. However, *R* sometimes may not necessarily indicate better performance due to the tendency of the model to deviate toward higher or lower values, especially when the data range is very wide and most of the data are distributed around their mean. Consequently, R^2 can be used as a more reliable indicator for measuring the model performance. R^2 demonstrates a degree of similarity between predicted and measured values, with R^2 values close to 1 indicating that the predicted and measured values are very similar. Low *BIAS* and *RMSE* values indicate high confidence in the developed model for prediction values. The analytical performance measures of the MARS

model in Table 3 demonstrate that the model performs well in both training and testing sets and the performance of MARS model for training set is consistent with testing sets.

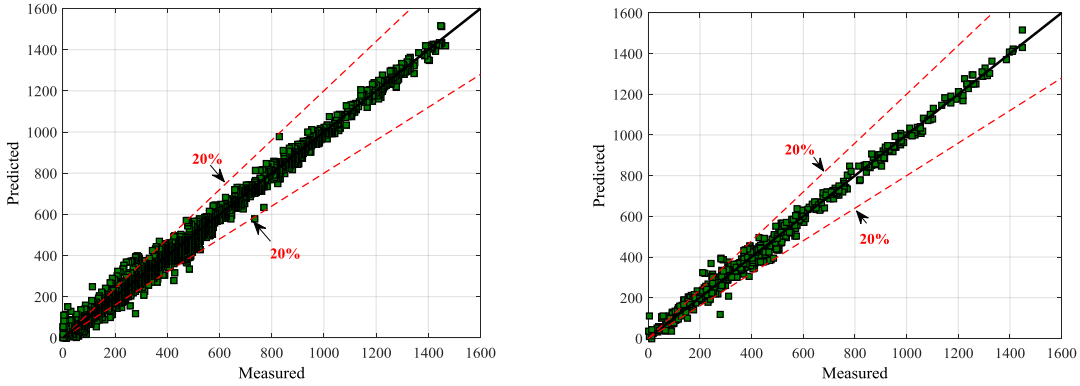

Figure 2. Comparison between measured and predicted values of drying shrinkage (a) Training, (b) Testing.

Table 3: The performances of developed MARS model for training and testing datasets.

Subsets	*BIAS*	*RMSE*	*R*	R^2
Training	1.53×10^{-5}	37.59	0.9931	0.9862
Testing	0.029	41.48	0.9919	0.9837

The performance of MARS model is also compared with several codes of practice including ACI [1], B3 [23], CEB MC90-99 [3], and GL2000 [4]. In order to evaluate the capabilities of MARS model, the BIAS, RMSE, R, R^2 statistical error measures were used [24]. The prediction performances of different models for entire database are presented in Table 4. For more visualization, Fig. 3 illustrates the histogram plots of the ratio of predicted drying shrinkage to experimentally measured values for the whole database. It can be concluded from Fig. 3 and Table 4 that the MARS model has provided significantly better results than other models.

Table 4: The comparison of MARS model with design codes

Model	R	R^2
ACI model	0.7842	0.6149
CEB model	0.9076	0.8238
GL2000 model	0.9277	0.8606
B3 model	0.9390	0.8818
MARS (this study)	0.9928	0.9857

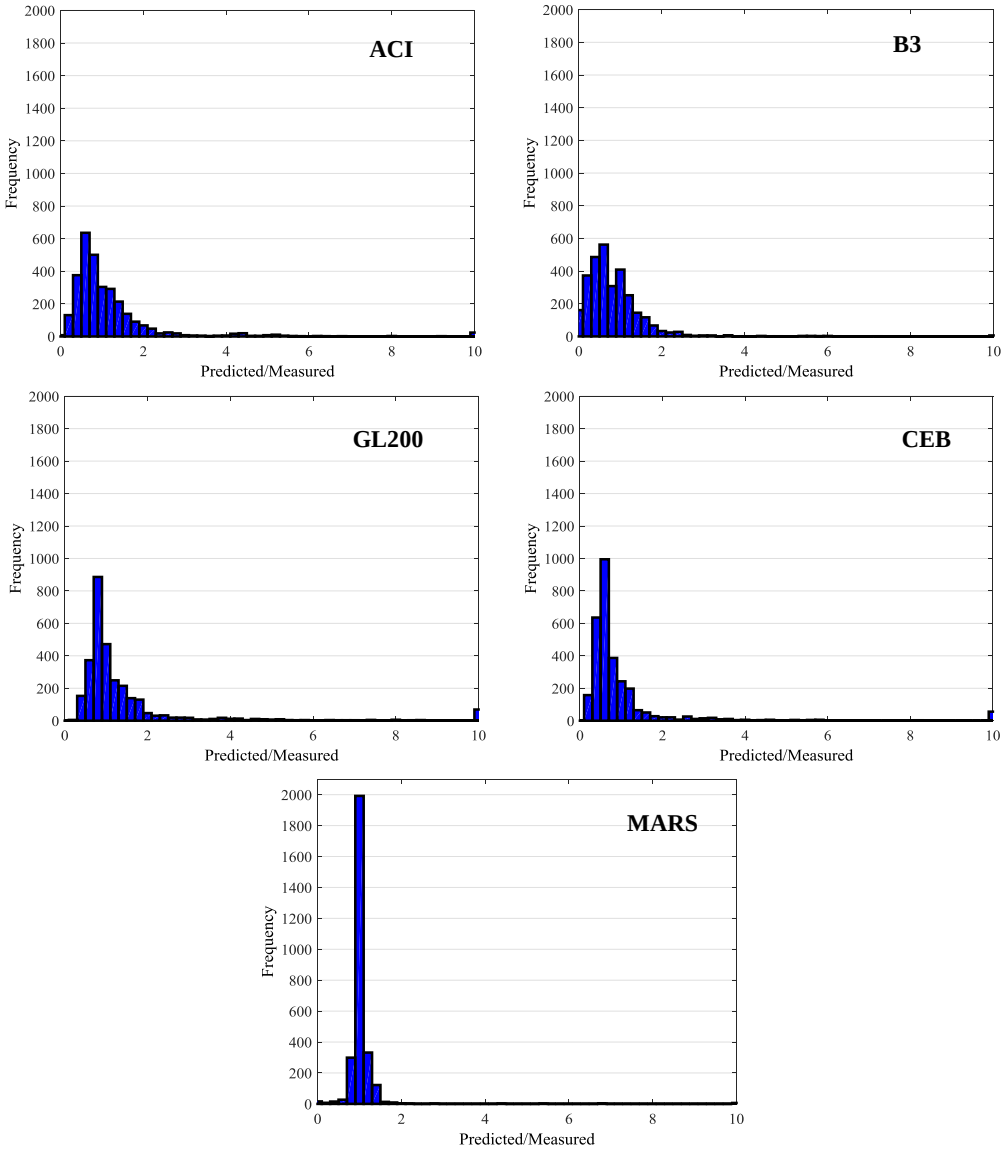

Figure 3. The histograms of the ratio between predicted and measured shrinkage for different models

3.3 Model robustness via sensitivity analysis and parametric study

One of the main advantages of the MARS model is its ability to determine whether a specific input parameter plays a crucial role in estimating output parameters or it only marginally improves the accuracy of the model [25]. Table 5 displays the analysis of variance (ANOVA) decomposition of the developed MARS model for estimating drying shrinkage. The first column lists the number of ANOVA function. The second column gives the standard deviation of corresponding ANOVA functions. This gives an indication of the relative contribution of each function to the overall model performance. The third column provides another indication of the importance of the corresponding ANOVA function, by listing the GCV score for a model including all basis functions compared to a model in

which that particular ANOVA function is removed. This can be used to judge whether this ANOVA function makes an important contribution to the model performance, or whether it only slightly improves the global GCV score. The last column gives the particular predictor variables associated with ANOVA function [22]. This ability of MARS can be employed to determine the relative importance of input parameters which are involved in estimation of drying shrinkage.

To more illustrate the sensitivity analysis based on GCV values, the results are schematically presented in Fig. 4. As shown, the contribution of W/C parameter in developing a predictive model based on MARS algorithm are more remarkable in comparison with other parameters. f_{cm28}, E_{cm28}, t, t_c, RH, C, V/S, and a/c are the other important parameters, respectively.

Table 5: The results of the analysis of variance (ANOVA) for the developed MARS model

Function number	STD	GCV	Variables	Function number	STD	GCV	Variables
1	4.098	48.752	1	17	0.012	0.001	1 7 8
2	0.294	0.100	4	18	0.356	0.154	1 8 9
3	0.185	0.164	6	19	0.049	0.004	2 6 8
4	3.145	61.825	8	20	0.004	0.001	2 8 9
5	8.897	129.906	1 4	21	0.369	0.182	3 4 6
6	0.106	0.032	1 5	22	0.091	0.012	3 6 8
7	0.069	0.006	1 8	23	0.285	0.097	3 7 8
8	6.660	112.431	1 9	24	0.143	0.024	4 6 9
9	0.057	0.007	2 8	25	1.774	4.498	1 3 4 9
10	0.079	0.005	6 8	26	0.037	0.003	1 4 6 9
11	0.057	0.005	6 8	27	0.026	0.002	1 4 8 9
12	3.362	15.546	6 9	28	0.270	0.086	3 6 7 8
13	3.133	13.531	7 8	29	0.007	0.001	3 7 8 9
14	0.882	1.149	1 3 4	30	0.011	0.001	4 6 8 9
15	0.543	0.374	1 4 8	31	0.100	0.014	1 3 4 5 9
16	4.806	32.037	1 4 9				

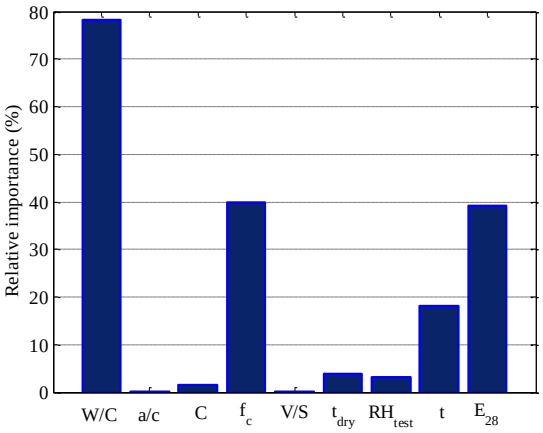

Figure 4. The result of sensitivity analysis

To ensure that the results of the developed model are in line with the physical concept of shrinkage problem, a parametric study is done. The main aim of the parametric study is to quantify the effect of each input parameter when all the other are fixed at their mean values. For instances, the variations of the drying shrinkage with C, W/C, and RH parameters for different ages are shown in Fig. 5. As shown in Fig. 5(a), the drying shrinkage increases as the cement content increases. The similar behavior is also observed for W/C parameter (see Fig. 5(b)). Furthermore, the amount of shrinkage is also more at greater ages. In Fig. 5(c), the variations of drying shrinkage with RH parameter are also shown. It can be seen from this figure that the shrinkage at lower ages decreases when the relative humidity increases. On the contrary, the shrinkage first increases small and then decreases at higher ages. These results are also reported in previous studies (e.g. [19]) and confirm the robustness of the developed model.

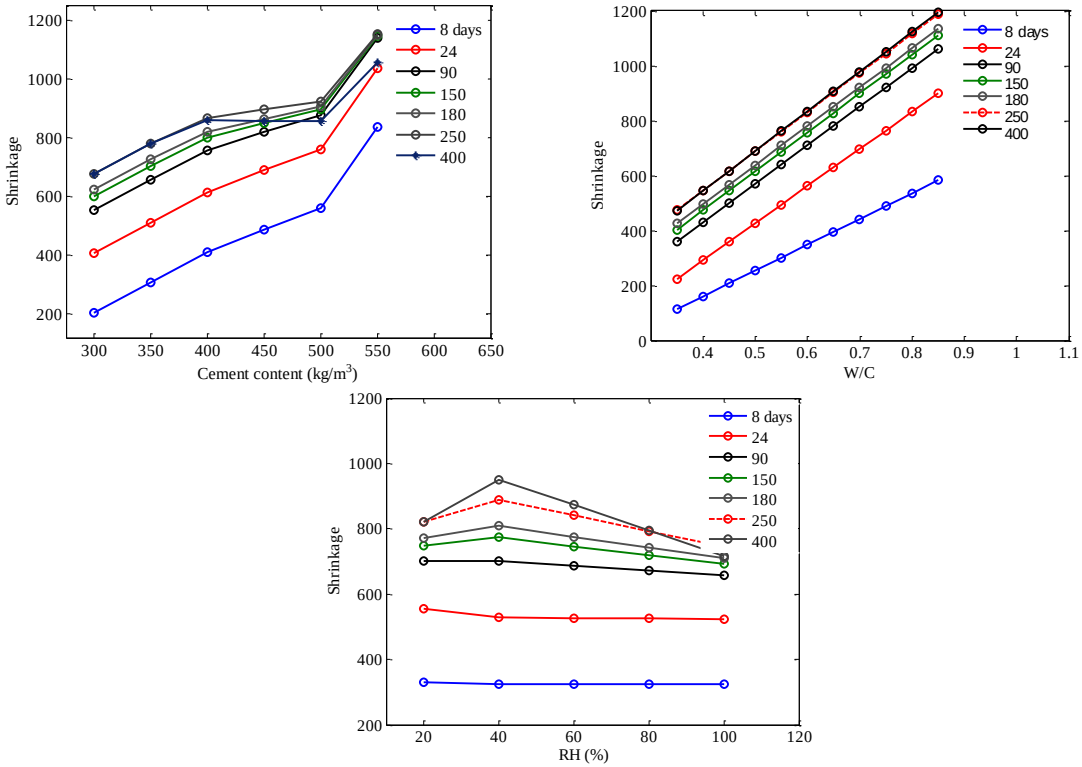

Figure 5. The results of parametric analysis

5. CONCLUSION

In the present study, a nonparametric and nonlinear approach namely the multivariate adaptive regression splines (MARS) is applied to predict the drying shrinkage of concrete. To achieve this, a comprehensive database from RIELM databank is used. Several influential parameters such as the age of onset of shrinkage measurement (t), age at start of drying (t_c), the ratio of the volume of the sample on its drying surface (V/S), relative

humidity (*RH*), cement content (*C*), the ratio of water content and cement content (*W/C*), the ratio of sand on total aggregate (*a/c*), average compressive strength at 28 days (f_{cm28}), and modulus of elasticity at 28 days (E_{cm28}) are considered as predictive parameters. The results of statistical error analysis indicate that the MARS model notably outperforms different codes of practice presented in the literature. The sensitivity analysis indicates that the W/C, f_{cm28}, and E_{cm28} are the main predictive parameters in the developed model. Furthermore, the results of parametric analysis verify the capability of the MARS model in capturing the physical trends between predictive variables and the drying shrinkage. In general, the results of parametric and sensitivity analyses confirm the robustness of the proposed MARS model for predicting the drying shrinkage.

REFERENCES

1. Committe A. Guide for Modeling and Calculating Shrinkage and Creep in Hardened Concrete, ACI Committe, 2008.
2. Recommendation RD, P.D.R. DE LA RILEM. Creep and shrinkage prediction model for analysis and design of concrete structures-model B3, *Mater Struct* 1995; **28**: 357-65.
3. Muller H, H Hilsdorf. Evaluation of the time-dependent behavior of concrete, summary report on the work of general task group 9, *CEB Bulletin d'Inform* 1990; **199**: 290.
4. Gardner N, Lockman M. Design provisions for drying shrinkage and creep of normal-strength concrete, *Mater J* 2001; **98**: 159-67.
5. Bažant ZP, Panula L. Practical prediction of time-dependent deformations of concrete, Part I: Shrinkage, *Matériaux et Construct* 1978, **11**: 307-16.
6. Bažant ZP, Panula L. Practical prediction of time-dependent deformations of concrete, Part II: Basic creep, *Matériaux et Construct* 1978, **11**: 317-28.
7. Bažant ZP, Panula L. Practical prediction of time-dependent deformations of concrete, Part III: Drying Creep, *Matériaux et Construct* 1978, **11**: 415-24.
8. Bažant ZP, Panula L. Practical prediction of time-dependent deformations of concrete, Part IV: Temperature effect on basic creep, *Matériaux et Construct* 1978, **11**: 424-34.
9. Bažant ZP, Kim JK. Segmental box girder: effect of spatial random variability of material on deflections, *J Struct Eng* 1991; **117**: 2542-47.
10. Bažant ZP, Kim JK. Improved prediction model for time-dependent deformations of concrete: Part 2—Basic creep, *Mater Struct* 1991; 24: 409-21.
11. Goel R, Kumar R, Paul D. Comparative study of various creep and shrinkage prediction models for concrete, *J Mater Civil Eng* 2007, **19**: 249-60.
12. Kaveh A, Hamze-Ziabari SM, Bakhshpoori T. M5' algorithm for shear strength prediction of hsc slender beams without web reinforcement, *Int J Model Optim* 2017; **7**: 48-53.
13. Kaveh A, Hamze-Ziabari SM, Bakhshpoori T. Patient rule-induction method for liquefaction potential assessment based on CPT data, *Bulletin Eng Geology Environ* 2016; 1-17.
14. Kaveh A, Bakhshpoori T, Hamze-Ziabari SM. New model derivation for the bond behavior of NSM FRP systems in concrete, *Iranian J Sci Technol*, 2017, 1-14.
15. Kaveh A, Bakhshpoori T, Hamze-Ziabari SM. Derivation of new equations for

prediction of principal ground-motion parameters using M5' algorithm, *J Earthq Eng* 2016; **20**: 910-30.
16. Kiani B, Gandomi AH, Sajedi S, Y. Liang R. New formulation of compressive strength of preformed-foam cellular concrete: an evolutionary approach, *J Mater Civil Eng* 2016; **28**: 04016092.
17. Gholampour A, Gandomi AH, Ozbakkaloglu T. New formulations for mechanical properties of recycled aggregate concrete using gene expression programming, *Construct Build Mater* 2017; **130**: 122-45.
18. Gandomi AH, Faramarzifar A, Rezaee PG, Asghari A, Talatahari S. New design equations for elastic modulus of concrete using multi expression programming, *J Civil Eng Manage* 2015, **21**: 761-74.
19. Bal L, Buyle-Bodin F. Artificial neural network for predicting drying shrinkage of concrete, *Construct Build Mater* 2013; 38: 248-54.
20. Friedman JH. Multivariate adaptive regression splines, *Annals Statist* 1991; 1-67.
21. http://www.civil.northwestern.edu/people/bazant/creepshrinkdata_20150511gb.xlsx.
22. Smith GN. *Probability Statistics Civil Engineering*, Collins Professional and Technical Books, (1986) 244.
23. Bazant ZP, Baweja S. Creep and shrinkage prediction model for analysis and design of concrete structures: Model B3, *ACI Special Publicat* 2000; **194**: 1-84.
24. Kaveh A, Hamze-Ziabari SM, Bakhshpoori T. Feasibility of pso-anfis-pso and ga-anfis-ga models in prediction of peak ground acceleration. International Journal of Optimization in Civil Engineering. 2018; 8 (1) :1-14
25. Kaveh Ali, Bakhshpoori T, Hamze-Ziabari SM. "M5'and Mars Based Prediction Models for Properties of Self-compacting Concrete Containing Fly Ash." *Periodica Polytechnica Civil Engineering*, 2017, 1-13.